Acta Biomaterialia 6 (2010) 3998–4004

Contents lists available at ScienceDirect

Acta Biomaterialia

journal homepage: www.elsevier.com/locate/actabiomat

Silica–collagen bionanocomposites as three-dimensional scaffolds for fibroblast immobilization

Martín F. Desimone [a,b], Christophe Hélary [a], Ivo B. Rietveld [c], Isabelle Bataille [d,e], Gervaise Mosser [a], Marie-Madeleine Giraud-Guille [a], Jacques Livage [a], Thibaud Coradin [a,*]

[a] UPMC Université Paris 06; CNRS, Chimie de la Matière Condensée de Paris, Collège de France, 11 place Marcelin Berthelot, F-75005 Paris, France
[b] IQUIMEFA-CONICET, Facultad de Farmacia y Bioquimica, Universidad de Buenos Aires, 1113 Buenos Aires, Argentina
[c] Université Paris Descartes, Faculté de Pharmacie, Chimie Physique – Case 23, F-75006 Paris, France
[d] INSERM, U698, CHU Xavier Bichat, Bât. Inserm, 46 rue Henri-Huchard, F-75018 Paris, France
[e] BPC, Institut Galilée, Université Paris 13, 93430 Villetaneuse, France

ARTICLE INFO

Article history:
Received 25 March 2010
Received in revised form 14 May 2010
Accepted 17 May 2010
Available online 21 May 2010

Keywords:
Collagen
Silica
Bionanocomposites
3-D culture
Fibroblasts

ABSTRACT

Silica–collagen bionanocomposite hydrogels were obtained by addition of silica nanoparticles to a protein suspension followed by neutralization. Electron microscopy studies indicated that larger silica nanoparticles (80 nm) do not interact strongly with collagen, whereas smaller ones (12 nm) form rosaries along the protein fibers. However, the composite network structurally evolved with time due to the contraction of the cells and the dissolution of the silica nanoparticles. When compared to classical collagen hydrogels, these bionanocomposite materials showed lower surface contraction in the short term (1 week) and higher viability of entrapped cells in the long term (3 weeks). A low level of gelatinase MMP2 enzyme expression was also found after this period. Several proteins involved in the catabolic and anabolic activity of the cells could also be observed by immunodetection techniques. All these data suggest that the bionanocomposite matrices constitute a suitable environment for fibroblast adhesion, proliferation and biological activity and therefore constitute an original three-dimensional environment for in vitro cell culture and in vivo applications, in particular as biological dressings.

1. Introduction

There is a current need for novel biological dressings, especially for treatment of burns and wound healing of chronic wounds such as foot ulcers [1–3]. In this context, collagen-based materials incorporating fibroblast cells appear highly promising due to their similarity with the dermis tissue [4,5]. However, the behaviour of fibroblasts within a three-dimensional (3-D) matrix strongly depends on the nature of the cell/material interactions and the stiffness of the gel. Immobilization of the cell within the gel usually triggers a series of physical (contraction) and biological responses to create a more suitable microenvironment, strongly impacting on the host material but also inducing cell phenotypic modifications [6–8]. Therefore, one of the main challenges in the area of skin tissue engineering and biological dressings is to design a cellularized material that (i) exhibits a suitable composition allowing cell adhesion on the surface of the internal cavities, and (ii) reaches a suitable stiffness to compensate for the contraction of the cell.

The established methods for producing collagen gels involve forming these at low collagen concentration, resulting in poor gel stiffness, and therefore strong and fast contraction [9]. Recently, a process has been developed that uses higher collagen concentrations, which limits gel contraction while enhancing cell activity [10]. In parallel, the addition of polymers, either natural or synthetic, or of inorganic particles was also studied but most of these works were performed on acellularized systems [11–13]. Recently, we have shown that hybrid materials made from collagen and silicates were efficient in decreasing gel contraction and enhancing cell proliferation in the short term [14]. However, in the longer term, reorganization of the collagen network and rapid silica dissolution occurred, to the detriment of cell activity.

Although several other routes to silica–collagen hybrid materials have been reported, none of them appeared compatible with the simultaneous encapsulation of fibroblasts [15–20]. Therefore, we developed an alternative, composite-like strategy to strengthen collagen gels with silica colloids, as already described for other biopolymer gels [21,22]. A combination of chemical and biological analyses was used to study the time evolution and final properties of the materials. All these analyses provide good evidence that silica–collagen bionanocomposites are suitable 3-D hosts for

* Corresponding author. Tel.: +33 144271528; fax: +33 144271443.
E-mail address: thibaud.coradin@upmc.fr (T. Coradin).

1742-7061/$ - see front matter © 2010 Acta Materialia Inc. Published by Elsevier Ltd. All rights reserved.
doi:10.1016/j.actbio.2010.05.014

fibroblast encapsulation, proliferation and activity, and may in the future be developed for in vitro 3-D culture models and for in vivo applications such as biological dressings.

2. Materials and methods

2.1. Fibroblast cell culture

Normal human dermal fibroblasts (Promocell) were propagated in Dulbecco's Modified Eagle's Medium (Gibco BRL) supplemented with 10% fetal calf serum (Gibco BRL), 100 units ml^{-1} penicillin, 100 μg ml^{-1} streptomycin (Gibco BRL) and 0.25 μg ml^{-1} Fungizone (Gibco BRL). Tissue culture flasks (75 cm^2) were kept at 37 °C in a 95% air and 5% CO_2 atmosphere. Before confluence, fibroblasts were removed from culture flasks by treatment with 0.1% trypsin and 0.02% EDTA. Cells were rinsed and resuspended in the above culture medium. Fibroblasts were used at passage 7 for the experiments. Collagen type I was purified from rat tails and the concentration was estimated by hydroxyproline titration [23].

2.2. Nanocomposite preparation

Silica nanoparticles 12 nm in size (Si12) (Ludox HS-40) were purchased from Aldrich. 80 nm silica nanoparticles (Si80) were synthesized by the Stöber method using ammonia for the base-catalyzed hydrolysis and polymerization of tetraethylorthosilicate [24]. Silica nanoparticle–collagen bionanocomposites with fibroblasts were prepared by mixing 0.6 ml of collagen solution (2.8 mg ml^{-1} in 17 mM acetic acid) with 0.8 ml of complete culture medium in an ice bath. In parallel, a suspension of nanoparticles was acidified to pH 3.0 with acetic acid. Precise amounts of the silica nanoparticle suspension were added to the collagen solution in order to obtain different final concentrations (5 and 10 mM) in the gels. The solution was then neutralized with 0.08 ml of 0.1 M NaOH and finally 0.6 ml of a cell suspension in complete medium supplemented with PBS was added. The cell density in each gel at the beginning of the experiments was 1×10^5 cells per gel. The reference classical collagen hydrogels (0.6 mg ml^{-1}) were prepared following the same protocol previously described by Bell [4] except that no silica nanoparticles were added.

2.3. Fibroblast viability

The cellular viability of entrapped cells was determined by the tetrazolium assay [25]. This colorimetric assay is based on the ability of the mitochondrial dehydrogenase enzymes of living cells to convert 3-(4,5-dimethyl-thiazol-2-yl)-2,5-diphenyl-tetrazolium bromide (MTT) into an insoluble formazan. In short, a 5 mg ml^{-1} solution of MTT in PBS was prepared and added to the immobilized cells, and then incubated at 37 °C in a humidified 5% CO_2 air atmosphere for 4 h. Afterwards, the MTT solution was removed, the gels washed three times with PBS and dimethyl sulfoxide was added. The optical density (OD) of the purple solution was read at 570 nm with a spectrophotometer. Cell-mediated contraction was evaluated by measuring the diameter of the samples every 7 days for 21 days.

2.4. Ultrastructural characterization

Samples for scanning electron microscopy (SEM) were fixed using 3.63% glutaraldehyde in 0.05 M sodium cacodylate buffer (pH 7.4) with 0.3 M saccharose for 1 h at 4 °C. Following fixation, samples were washed three times in the same buffer and then dehydrated in a graded series of ethanol (70%, 95% and two changes of alcohol 100%). Finally, the samples were subjected to supercritical drying and were gold sputter-coated for analysis using a JEOL JSM 5510LV microscope operating at 10 kV. For transmission electron microscopy (TEM), following fixation and wash as described above, the samples were post-fixated using 2% osmium tetraoxide in 0.05 M sodium cacodylate buffer (pH 7.4) with 0.3 M saccharose for 1 h at 4 °C. Samples were then washed three times in the same buffer, dehydrated with ethanol and embedded in araldite. Thin araldite transverse sections (70–80 nm) were made with an Ultracut ultramicrotome (Reichert, France) and contrasted by phosphotungstic acid. Slides were then analyzed with a Philips CM12 electron microscope operating at 120 kV.

2.5. Differential scanning calorimetry (DSC)

DSC experiments were performed using a Mettler-Toledo (Switzerland) 822e thermal analyzer equipped with a Huber (Germany) TC100 cooling device for measurements down to –80 °C. Indium (T_{fus} = 156.60 °C, DH_{fus} = 3267 J mol^{-1}) and zinc (T_{fus} s = 419.53 °C, DH_{fus} = 7320 J mol^{-1}) were used for calibration of temperature. The initial samples were concentrated by removing about 50% of the water content. They were introduced into standard Mettler-Toledo 40 μl aluminum capsules and weighed on a microbalance sensitive to 0.01 mg.

2.6. Rheological measurements

Shear oscillatory measurements on nanocomposite disks were performed on a Bohlin Gemini rheometer (Malvern) equipped with plane acrylic 40 mm diameter geometry. Both base and geometry surfaces were rough in order to avoid sample slipping during measurements. All tests were performed at 37 °C. Mechanical spectra, i.e. storage, G′ and loss, G″ modulus vs. frequency, were recorded at an imposed 1% strain, which corresponded to non-destructive conditions, as previously checked (data not shown). In order to test all nanocomposite materials under the same conditions, before each run the gap between base and geometry was chosen so that a slight positive normal force was applied to the gels during measurements. Four samples of each hydrogel type were tested at day 1.

2.7. MMP2 activity

Gelatin zymography was carried out using the Miniprotean III system (Bio-Rad), using a previously reported procedure [26]. Polyacrylamide migration gel was performed at 10% (ratio acrylamide/bis-acrylamide 37:1) in 0.375 M Tris–HCl, pH 8.8, containing 1 mg ml^{-1} gelatin and 0.1% sodium dodecyl sulfate (SDS). Stacking gel contained 4% polyacrylamide in 0.125 M Tris, pH 6.8, and 0.1% SDS. Gels were polymerized by adding 50 μl of 10% ammonium persulfate and 10 μl of 0.1% TEMED. At each culture time point, supernatants were half-diluted in 0.125 M Tris, pH 6.8, 50% glycerol, 0.4% bromophenol blue and deposited within gel wells (n = 3). Then, gels were run under Laemmli conditions (24 mM Tris, 192 mM glycine, 3.47 mM SDS; 40 mA, 1 h). Following electrophoresis, gels were washed twice (30 min each) in 200 ml of 2.5% Triton X-100 under constant mechanical stirring and then incubated in 100 mM Tris–HCl, pH 7.4, 30 mM $CaCl_2$ for 19 h at 37 °C. Gels were stained with Coomassie Blue R-250 for 2 h (50% methanol, 10% acetic acid) and destained appropriately (40% ethanol, 10% acetic acid). Proteinase activity was evidenced as cleared area. Finally, the gels were rinsed for 1 h in 5% ethanol, 7.5% acetic acid and kept in sealed bags containing distilled water. The stained polyacrylamide gels were observed with a CFR 126 Video camera and black and white images were converted into different gray levels. Complete digestion of gelatin substrate corresponded to a gray level of 255 and absence of digestion corresponded to a 0 gray level. The average surface of each lysis band from gelatin zymograms

was determined semi-automatically following its contour with a calibrated electronic slide on a BIOCOM station. Gelatinase activity was expressed as arbitrary units. A control was performed with culture medium collected on a collagen hydrogel without fibroblast. Results were normalized by the MTT assay and expressed as the average value ± SD for each culture time point and compared to collagen hydrogels at day 7.

2.8. Histological analysis and immunodetection of collagen III, MMP1 and MT1-MMP

Sections 10 μm thick, transverse to the sample surface, were cut with a manual microtome (Stiassnie France). Paraffin sections were then rehydrated and stained with hemalun. The sections were dehydrated, mounted between slide and coverslip, and observed with an optical microscope (Nikon E600 POL). Photographs of hydrogel slides were taken with a CCD camera (Nikon). For indirect immunodetection, after rehydration and an extended wash in PBS, the rehydrated sections were incubated 5 min at room temperature with 0.2% pepsin in acetic acid 10% (v/v). The sections were rinsed in PBS and incubated for 30 min in PBS containing 1% glycin. After another wash in PBS, the sections were incubated 60 min at room temperature with a blocking solution (0.05% Tween PBS, 1% bovine serum albumin, 10% calf serum). Adequate dilutions of primary antibodies against collagen III, MMP1 or MT1-MMP (1/50 and 1/10 dilution, respectively) were added to different sections and incubated in a moist chamber overnight. The following day, sections were incubated in a moist and dark chamber for 90 min with a secondary antibody anti-mouse coupled with Rhodamine (Molecular Probes). After three rinses in PBS, sections were then incubated for 10 min in a DAPI bath (dilution: 1/50,000 v/v). Finally, slides were rinsed three times in PBS and observed with an AXIO 100 (Zeiss) fluorescence microscope.

3. Results

3.1. Silica–collagen nanocomposite materials

When fibroblasts are entrapped within collagen hydrogels, they pull the collagen fibrils to enhance the density, and therefore the stiffness, of their environment. This results in a contraction of the gel that can be quantified by measuring the decrease in gel surface. For classical collagen hydrogels, the surface rapidly decreases to 57% after 1 day and becomes 10% or less of the initial surface after 2 weeks (Fig. 1). The addition of silica nanoparticles efficiently delays the contraction process over the same period, with 76% of the initial surface found at day 1 for 10 mM Si80 addition and 49% at day 7 for 10 mM Si80 and Si12 (compared to 23% for classical collagen hydrogels). At day 14, the lowest contraction is observed for 10 mM Si12 (22% compared to 10% for reference gels). In all cases, lower silica nanoparticle concentration (5 mM) leads to larger, or at best equivalent, contraction.

In parallel, the structural evolution of the composite gel was followed by SEM and TEM (Fig. 2a and b). After 1 day, SEM images indicate that the classical collagen gels consist of a highly porous structure formed by thin homogeneous collagen fibrils with a diameter of about 50 nm (Fig. 2a;A). This characteristic structure was also observed in silica nanoparticle–collagen gels (Fig. 2a;B and C). TEM further confirms the SEM observations and shows that the characteristic collagen cross-striations were visible in all conditions (Fig. 2b;A–C), indicating that the addition of silica nanoparticles to the acid collagen solution did not modify the self-assembly of collagen molecules to form organized supramolecular fibrils after neutralization. In addition, Si12 nanoparticles are organized as necklaces, suggesting that they surround the collagen molecules (Fig. 2b;B). Such an organization is not seen for Si80 nanoparticles that nevertheless seem systematically associated with collagen fibrils within the gel network (Fig. 2b;C). After 3 weeks, a local but limited aggregation of collagen fibrils was observed by SEM in classical collagen gels, due to cell contraction activity (Fig. 2a;D). A similar evolution was observed for Si80 nanoparticle addition (Fig. 2a;F). In contrast, larger fibrils aggregates are apparent in the presence of Si12 colloids (Fig. 2a;E). These phenomena are also visible on the TEM images where collagen fibrils appear more entangled with one another (Fig. 2b;D). In addition, the density of Si12 is apparently lower after this delay (Fig. 2b;E). In the case of Si80, particles much smaller than the original ones are visible after 3 weeks in the vicinity of collagen fibers (Fig. 2b;F). As both situations may result from silica dissolution, the release of silica from the composite gels was investigated by Si titration using inductively coupled plasma atomic emission spectroscopy (ICP-AES) on the gel supernatant. This release was initially slightly faster for the Si80–collagen gels during the first 14 days, but at the end of the 21 days the released amount ranged from 35% to 45% for all samples (Fig. 3).

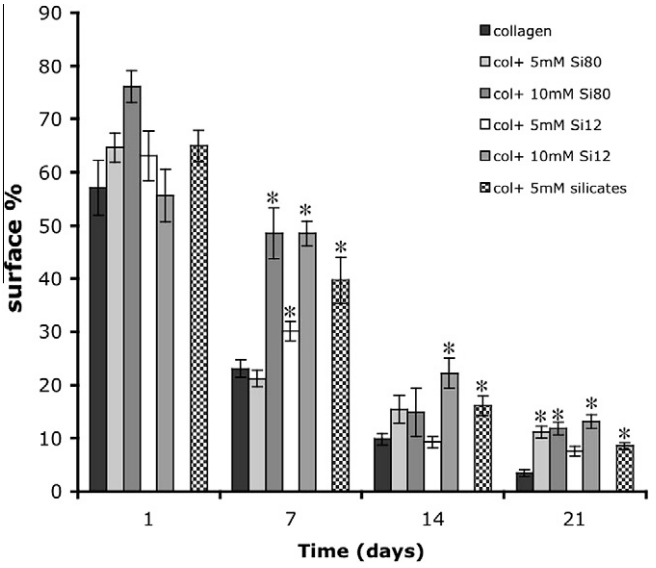

Fig. 1. Cell-mediated contraction of the nanoparticle–collagen nanocomposites. Results are expressed as mean ± SD from triplicate experiments. *Statistical significance ($P < 0.05$) according to Student's test.

Composite materials obtained in the absence of cells were studied by DSC and rheology. The peak temperature for collagen denaturation was found at 55 °C for pure collagen and did not change significantly when silica nanoparticles, irrespective of their size and concentration, were present in the system (Fig. 4a). Mechanical properties were also analysed for the 10 mM nanoparticle–collagen nanocomposites showing that both storage and loss moduli, G′ and G″, increased in Si12–collagen nanocomposites; Si80–collagen gels did not present a significant difference when compared to the control collagen hydrogels (Fig. 4b).

3.2. Encapsulated fibroblast behaviour

The viability of fibroblasts within silica nanoparticles–collagen gels was first studied using the MTT assay. In classical collagen hydrogels, fibroblast viability increased by a factor of 2 within the first week and then remained constant. The largest silica particles, Si80, appear to have the most noticeable effect, independent of their concentration, particularly after 2 and 3 weeks where a 6-fold increase in activity is observed compared to the control

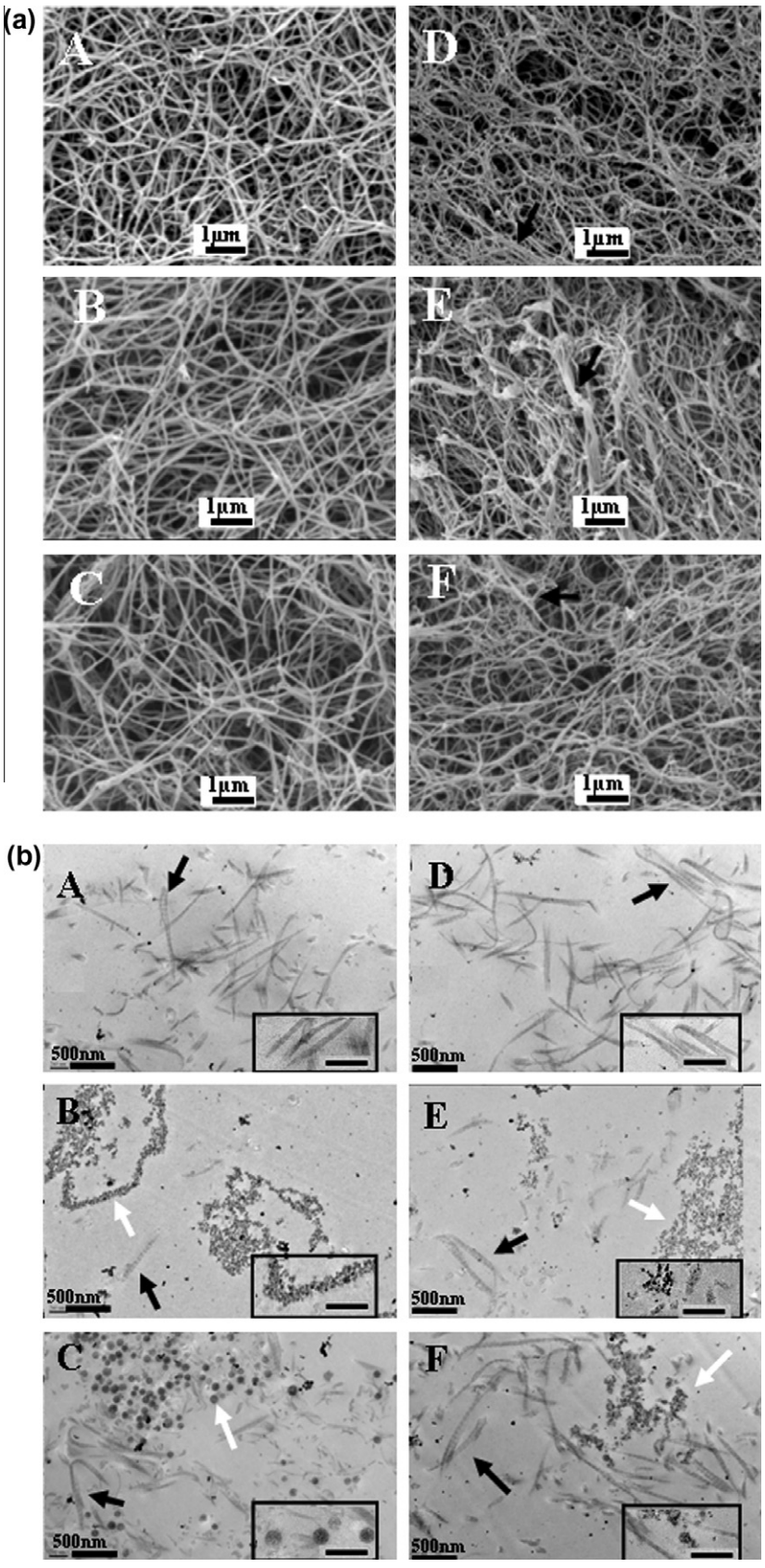

Fig. 2. Representative (a) SEM and (b) TEM images of collagen (top line), Si12–collagen (middle line) and Si80–collagen (bottom line) hydrogels after incubation for 1 day (A–C) and 21 days (D–F) (insert scale bar 200 nm). In the SEM images, dark arrows show local fiber aggregation. In the TEM images, dark arrows show collagen fibrils and white arrows show silica nanoparticles.

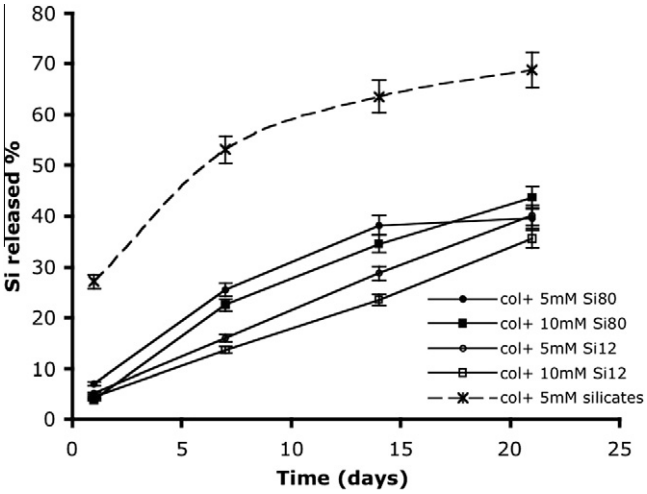

Fig. 3. Si released from hybrid bionanocomposite gels.

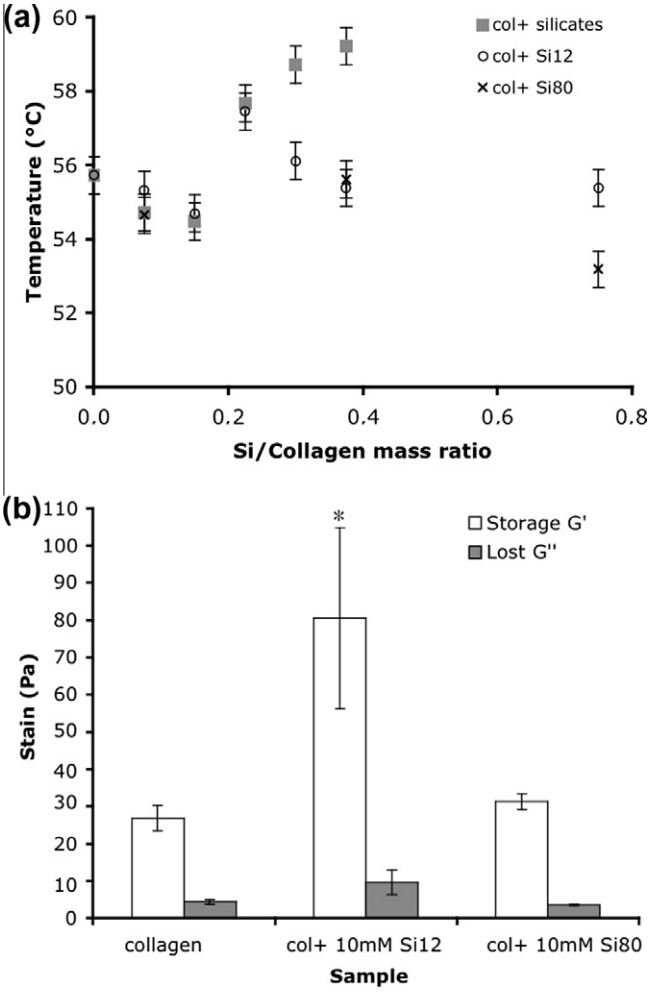

Fig. 4. Effect of silica addition on (a) the denaturation temperature of collagen and (b) the storage (G′) and loss (G″ moduli of selected materials.

(Fig. 5). The smaller Si12 colloids also clearly enhance cell metabolic activity on the long term but to a lesser extent (up to three times compared to pure collagen after 21 days).

After entrapment, fibroblast cells may undertake remodelling of the gel structure, starting with collagen degradation. This degradation can be monitored by studying the activity of MMP2 enzyme (Fig. 6) [27]. MMP2 activity was detected after 7 days for each material, except in the 10 mM Si12–collagen gels. At this time, the activity was lower in silicified gels than in reference collagen gels. With time, the collagen degradation activity of the entrapped cells increased progressively for classical hydrogels. In contrast, the active form of MMP2 was present at significantly lower levels in all composite materials, and after 3 weeks, presented 3-fold lower activity levels than the control collagen gel.

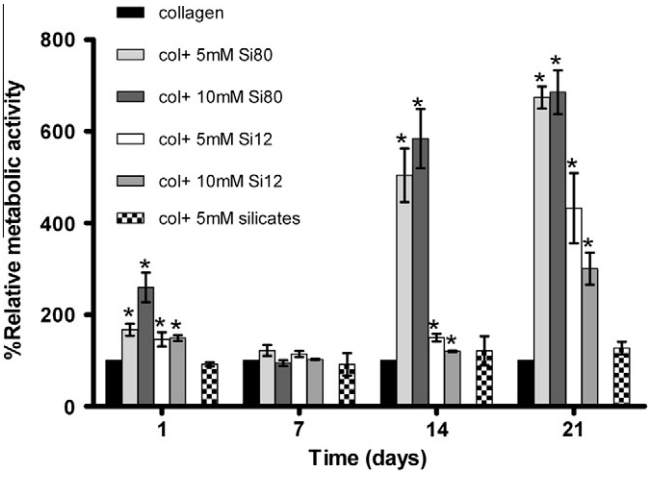

Fig. 5. Metabolic activity of entrapped fibroblasts (MTT assay). Control collagen hydrogels were normalized to 100% at each time point. Results are expressed as mean ± SD from triplicate experiments. *Statistical significance ($P < 0.05$) according to Student's test.

As these two techniques suggested that the composite networks were suitable environments for cell proliferation, their response to encapsulation was further examined qualitatively in terms of cell distribution and morphology by histology analysis as well as immunolabelling techniques (Fig. 7). Optical microscopy inspection of the samples indicated that the cells were able to spread and proliferate in the core regions of the bionanocomposites. In all cases, homogeneous distributions of the cells with a spindle shape were observed. Moreover, these results confirm the presence of an interconnected pore network capable of ensuring a good

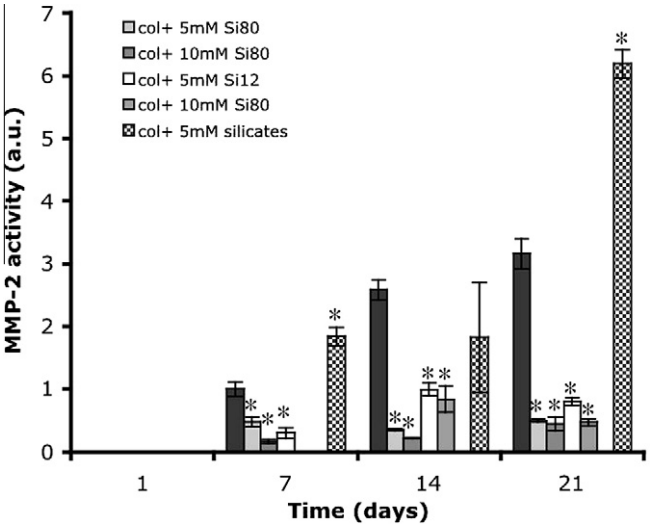

Fig. 6. Catabolic activity of entrapped fibroblasts (active form of the MMP2 enzyme produced by the cells normalized to MTT assay). Results are expressed as mean ± SD from triplicates experiments. *Statistical significance ($P < 0.05$) according to Student's test.

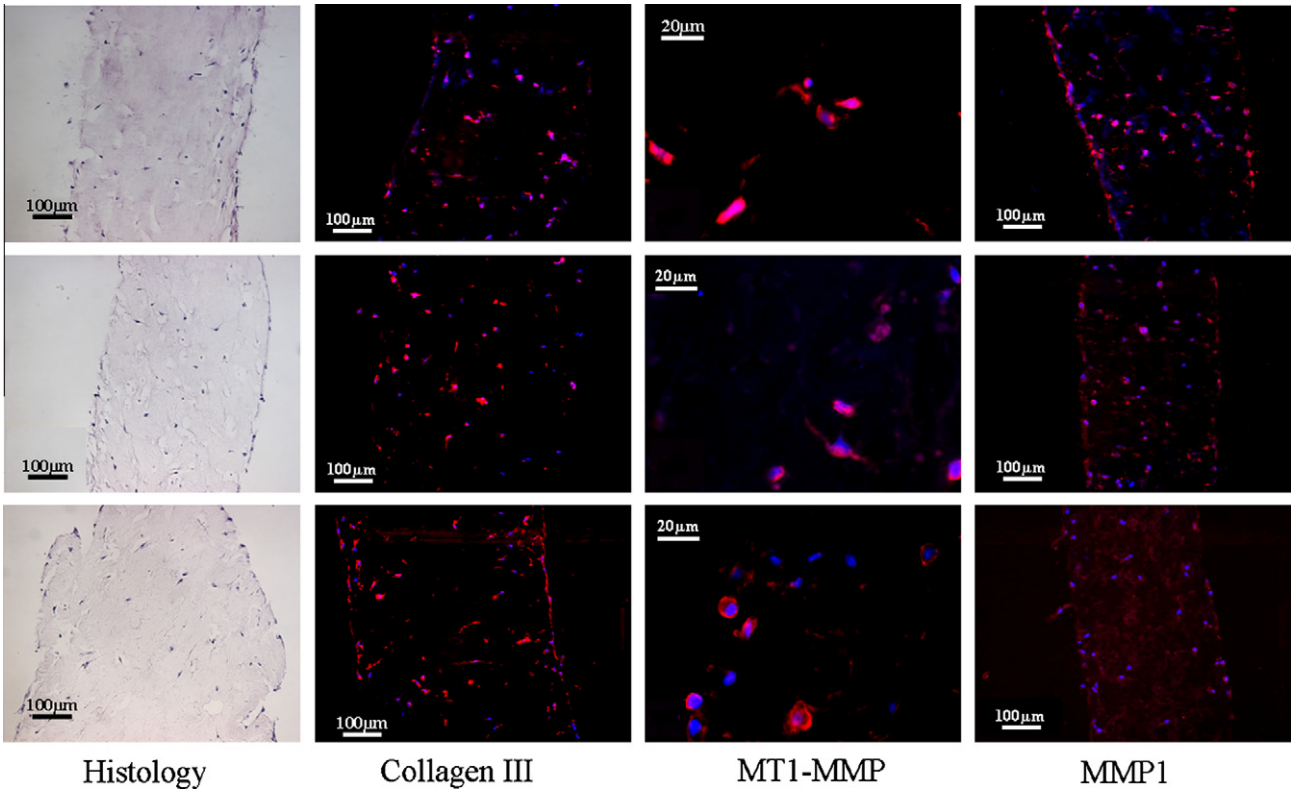

Fig. 7. Representative images of histology and immunodetection of collagen III, MT1 and MMP1 of collagen (top line), Si80–collagen (middle line) and Si12–collagen (bottom line) hydrogels after incubation for 21 days.

mass transfer of nutrients and waste products, which is an important issue in tissue engineering. The immunodetection of the MT1-MMP collagenase [28], which is responsible for the activation of the MMP2, as well as that of MMP1, which hydrolyses collagen, suggests that these enzymes are present in all the materials. Although this technique is only qualitative, it is worth noting that within classical hydrogels, only the red fluorescent signal of the membrane-bound MT1-MMP is observed, whereas in bionanocomposite hydrogels, the blue fluorescence corresponding to cell nucleus is much more visible, suggesting lower levels of MT1-MMP expression, in agreement with MMP2 activity measurements. In addition, it was possible to detect collagen III [29], a good marker for newly synthesized collagen fibrils resulting from the anabolic activity of the cells, in all samples.

4. Discussion

The first aim of silica nanoparticle addition to collagen hydrogels was to improve their resistance to cell contraction activity in order to enhance cell proliferation. Rheological measurements of acellularized materials indicate that collagen and Si80–collagen composites exhibit similar stiffness, while Si12–collagen composites are slightly stiffer. However, these variations are small, suggesting rather weak silica–collagen interactions This is supported by the absence of significant variation in collagen thermal stability, as obtained from DSC measurements. SEM images also indicate that silica addition does not initially modify the initial structure of the collagen network, although TEM images suggest that nanoparticles are in close proximity to the collagen fibrils.

Despite these limited effects, addition of silica nanoparticles to collagen gels has a significant effect on the time evolution of the gel structure and the cellular activity, and two different periods may be distinguished. Over the first week, a strong contraction step occurs where cells mainly modify their environment, especially via collagen fibril network remodelling [6–8]. During this stage, cell viability, MMP2 production and gel surface contraction are clearly correlated when considering the effect of silica nanoparticle size and concentration. It was suggested that during the time when fibroblasts are migrating, attaching to and spreading on collagen matrices, the contractile forces they generate are force-limited and not displacement-limited [30]. In other words, cells are able to adapt the number and spatial distribution of focal adhesion sites, via cell elongation and migration, in order to develop a suitable level of force. Therefore the gel contraction process depends not only on the possibility for collagen fibrils to aggregate for a similar cell contraction activity (material stiffness) but also on the cell/material contact interactions (material composition).

In this context, TEM suggests that some of the fibrils are densely covered by Si12 rosaries, while, at a similar concentration, Si80 nanoparticles appear more disperse. This suggests that for classical collagen hydrogels where fibroblast/matrix adhesion contacts are good and inter-fibril sliding during contraction is easy, the suitable adhesion that should be beneficial for cell activity does not compensate for the poor resistance to cell contraction, which occurs too rapidly and becomes detrimental to cell activity. For Si12–collagen composites, both cell adhesion and fibril aggregation are limited by the presence of a dense silica coating, so that the beneficial effect of an increase in material stiffness is offset by the poorer cell/matrix interactions. Si80 appears as an intermediate interesting situation where the presence of silica may be less detrimental to cell adhesion while limiting fibril aggregation.

After 21 days, all composites showed similar gel surface and cell MMP2 activity, respectively higher and lower than for reference collagen gels that have become almost independent of the initial silica content and size. At the same time, immunodetection of collagen III in all samples indicates that cells produce new collagen, a

good indication of their anabolic activity. This suggest that fibroblasts have entered a second stage where they can proliferate. However, a lower level of production of MT1-MMP and MMP1 is observed in the composites compared to the collagen gels, suggesting that the former materials represent a better environment for the cells compared to the latter.

In addition, fibroblasts immobilized in Si80–collagen materials still exhibit a significantly higher viability compared to Si12-based composites after 21 days. After this delay, about one-third of the initial amount of silica has been released, leading to a decrease in Si12 density and Si80 average particle size, as seen from TEM. In parallel, SEM observations show that the Si12–collagen materials exhibit larger fibril aggregates compared to Si80-based composites, which may constitute a less favourable situation for cell adhesion and proliferation.

Finally, it is interesting to compare these results with previous data on silica–collagen hybrid materials [14]. On the one hand, these materials were obtained by in situ polymerization of silicates, resulting in a continuous coating of collagen by silica. As a result, a significant increase in collagen thermal stability is observed and, in terms of gel contraction, a 5 mM silicate concentration has a similar effect as a 10 mM silica colloid content, at least in the short term. On the other hand, the strong reactivity of silicates towards collagen prevents their incorporation at concentrations higher than 5 mM. Moreover, they have a very strong influence on the aggregation of collagen fibrils under contraction, resulting in much lower cell viability and higher MMP2 production. Finally, due to their high solubility in biological media [31,32], silicates are almost fully released from the gel after 1 week.

5. Conclusions

The colloidal silica–collagen composites described in this paper are compatible with fibroblast cell encapsulation, and, when compared to classical collagen hydrogels, favour their viability while limiting gel contraction. They therefore constitute original 3-D environments for in vitro cell culture studies. In parallel, in vivo studies of their biocompatibility [33,34] are now underway in order to evaluate the potential of these composites as biological dressings [1–3].

Acknowledgements

M.F.D. thanks the Collège de France for funding and C. Illoul and A. Anglo (LCMCP) for their help with microscopy sample preparation. D. Talbot (PECSA, UPMC-P6) is kindly acknowledged for her collaboration with the ICP-AES measurements.

Appendix A. Figures with essential colour discrimination

Certain figures in this article, particularly Figure 7, are difficult to interpret in black and white. The full colour images can be found in the on-line version, at doi:10.1016/j.actbio.2010.05.014.

References

[1] Jones I, Currie L, Martin R. A guide to biological skin substitutes. Br J Plast Surg 2002;55:185–93.
[2] Ehrenreich M, Ruszczak Z. Update on tissue-engineered biological dressings. Tissue Eng 2006;12:2407–24.
[3] Metcalfe AD, Ferguson MWJ. Bioengineering skin using mechanisms of regeneration and repair. Biomaterials 2007;28:5100–13.
[4] Drury JL, Mooney DJ. Hydrogels for tissue engineering: scaffold design variables and applications. Biomaterials 2003;24:4337–51.
[5] Wong T, McGrath JA, Navsaria H. The role of fibroblasts in tissue engineering and regeneration. Br J Dermatol 2007;156:1149–55.
[6] Fluck J, Querfeld C, Cremer A, Niland S, Krieg T, Sollberg S. Normal human primary fibroblasts undergo apoptosis in three-dimensional contractile collagen gels. J Invest Dermatol 1998;110:153–7.
[7] Hadjipanayi E, Mudera V, Brown RA. Close dependance of fibroblast proliferation on collagen scaffold matrix stiffness. J Tissue Eng Regen Med 2008;3:77–84.
[8] Berry CC, Shelton JC, Lee DA. Cell-generated forces influence the viability, metabolism and mechanical properties of fibroblast-seeded collagen gel constructs. J Tissue Eng Regen Med 2009;3:43–53.
[9] Bell E, Ivarsson B, Merrill C. Production of a tissue-like structure by contraction of collagen lattices by human fibroblasts of different proliferative potential in vitro. Proc Natl Acad Sci USA 1979;76:1274–8.
[10] Hélary C et al. Concentrated collagen hydrogels as dermal substitutes. Biomaterials 2010;31:481–90.
[11] Chen G, Ushida T, Tateishi T. Hybrid biomaterials for tissue engineering: a preparative method for PLA or PLGA-collagen hybrid sponges. Adv Mater 2000;12:455–7.
[12] Rezwan K, Chen QZ, Blaker JJ, Boccaccini AR. Biodegradable and bioactive porous polymer/inorganic composite scaffolds for bone tissue engineering. Biomaterials 2006;27:3413–31.
[13] Sisco PN, Wilson CG, Mironova E, Baxter SC, Murphy CJ, Goldsmith EC. The effect of gold nanorods on cell-mediated collagen remodeling. Nano Lett 2008;8:3409–12.
[14] Desimone MF, Hélary C, Mosser G, Giraud-Guille MM, Livage J, Coradin T. Fibroblast encapsulation in hybrid silica/collagen hydrogels. J Mater Chem 2010;20:666–8.
[15] Ono Y, Kanekiyo Y, Inoue K, Hojo J, Nango M, Shinkai S. Preparation of novel hollow fiber silica using collagen fibers as a template. Chem Lett 1999;12:475–6.
[16] Coradin T, Giraud-Guille MM, Hélary C, Livage J, Sanchez C. A novel route to collagen–silica biohybrids. Mater Res Soc Symp Proc 2002;726:79–83.
[17] Eglin D, Mosser G, Giraud-Guille MM, Livage J, Coradin T. Type I collagen, a versatile liquid crystal biological template for silica structuration from nano- to microscopic scales. Soft Matter 2005;1:129–31.
[18] Eglin D, Shafran KL, Livage J, Coradin T, Perry CC. Comparative study of the influence of several silica precursors on collagen self-assembly and of collagen on 'Si' speciation and condensation. J Mater Chem 2006;16:4220–30.
[19] Heinemann S, Heinemann C, Ehrlich H, Meyer M, Baltzer H, Worch H, et al. A novel biomimetic hybrid material made of silicified collagen: perspectives for bone replacement. Adv Eng Mater 2007;9:1061–8.
[20] Heinemann S, Heinemann C, Bernhardt R, Reinstorf A, Nies B, Meyer M, et al. Bioactive silica–collagen composite xerogels modified by calcium phosphate phases with adjustable mechanical properties for bone replacement. Acta Biomaterialia 2009;5:1979–90.
[21] Darder M, Aranda P, Ruiz-Hitzky E. Bionanocomposites: a new concept of ecological bioinspired and functional hybrid materials. Adv Mater 2007;19:1309–19.
[22] Coradin T, Allouche J, Boissière M, Livage J. Sol–gel biopolymer/silica nanocomposites in biotechnology. Curr Nanosci 2006;2:219–30.
[23] Bergman I, Loxley R. Two improved and simplified methods for the analysis of hydroxyproline in tissues and urine. Anal Chem 1963;35:1961–5.
[24] Stöber W, Fink A, Bohn E. Controlled growth of monodisperse silica spheres in micron size range. J Colloid Interface Sci 1968;26:62–9.
[25] Mosmann T. Rapid colorimetric assay for cellular growth and survival: application to proliferation and cytotoxicity assays. J Immunol Methods 1983;65:55–63.
[26] Hélary C, Foucault-Bertaud A, Godeau G, Coulomb B, Giraud-Guille MM. Fibroblast populated dense collagen matrices: cell migration cell density and metalloproteinases expression. Biomaterials 2005;26:1533–43.
[27] Le J, Rattner A, Chepda T, Fray J, Chamson A. Production of matrix metalloproteinase 2 in fibroblast reaction to mechanical stress in a collagen gel. Arch Dermatol Res 2002;294:405–10.
[28] Zigrino P, Drescher C, Mauch C. Collagen-induced proMMP-2 activation by MT1-MMP in human dermal fibroblasts and the possible role of $\alpha 2\beta 1$ integrins. Eur J Cell Biol 2001;80:68–77.
[29] Mauch C, Hatamochi A, Scharffetter K, Krieg T. Regulation of collagen synthesis in fibroblasts within a three-dimensional collagen gel. Exp Cell Res 1988;178:493–503.
[30] Freyman TM, Yannas IV, Yokoo R, Gibson LJ. Fibroblast contractile force is independent of the stiffness which resists the contraction. Exp Cell Res 2002;272:153–62.
[31] Bass JD, Grosso D, Boissière C, Belamie E, Coradin T, Sanchez C. The stability of mesoporous oxide and mixed-metal oxide materials under biologically relevant conditions. Chem Mater 2007;19:4349–56.
[32] Finnie KS et al. Biodegradability of sol–gel silica microparticles for drug delivery. J Sol-Gel Sci Technol 2009;49:12–8.
[33] Radin S, El-Bassyouni G, Vresilovic EJ, Schepers E, Ducheyne P. In vivo tissue response to resorbable silica xerogels as controlled release materials. Biomaterials 2005;26:1043–52.
[34] Carturan G, Dal Toso R, Boninsegna S, Dal Monte R. Encapsulation of functional cells by sol–gel silica: actual progress and perspectives in cell therapy. J Mater Chem 2004;14:2087–98.